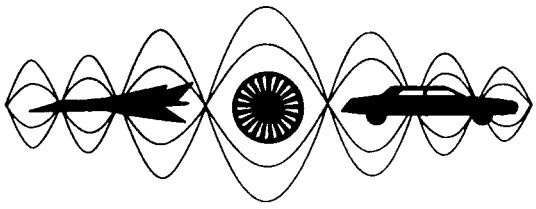

FIFTH INTERNATIONAL CONGRESS ON SOUND AND VIBRATION
DECEMBER 15-18, 1997
ADELAIDE, SOUTH AUSTRALIA

RANDOM VIBRATION OF ENGINE-MOUNTING SYSTEM WITH MOTION-LIMITING STOPS

AISAKA Masaharu(*) YOKOMICHI Isao(**) ARAKI Yoshiaki(***) INOH Takeshi(*)

(*)ISUZU Motors Ltd. Vehicle Research & Experiment Dept., Japan
(**)Kitakyusyu College of Technology, Dept. of Mech. Eng., Japan
(***)Kyusyu Institute of Technology, Dept. of Control Eng., Japan

This paper presents some results of a theoretical study of random impact vibrations of the engine-mounting system of heavy-duty trucks. The dynamic model of a vehicle is reduced to five degree-of-freedom system equipped with stoppers to limit the engine-body movement when traveling on rough roads. The impact force is reduced to the linear restoring and damping forces using by statistically equivalent coefficients of stiffness and damping. The responses of the system to road surface undulations are determined from the moment equation. These theoretical results are confirmed by the digital simulation.

1. Introduction

Recently, many successful improvements have been made in riding comfort and the strength of heavy-duty trucks. As an improvement for riding comfort, using an engine-body as dynamic vibration absorber has become known[1,2]. This application will decrease the beaming vibration of rudder frame arising from the tires run out at a certain vehicle velocity.

Heavy-duty trucks are featured with diversified wheel bases and bodies, resulting in differences in body-frame vibration characteristics. In case of low frequency characteristics, engine-mounting is set up with low stiffness for tuning with the engine body as the dynamic vibration absorber. In this case, it is necessary to install stoppers to limit the engine-body movement when traveling on rough roads. This paper deals with the strength problem of the engine-mounting system which is often caused the impact force from the rough roads.

This study presents an approximate analysis of random impact vibrations of the engine-mounting system. A closed form expression for moment equation can be obtained using the equivalent linear model of impact force which is given by minimizing the mean-square error between nonlinear and linear models. The influence of the stopper clearance on the impact force and the responses of the vibration can be determined. The digital simulation confirms the validity of these analytical results.

2. Nomenclature

A : Expanded matrix of (12 × 12)'s
B_f, B_r : Column vector of (12 × 1)'s
c_2, c_5 : Damping coefficient of front and rear suspensions
c_3 : Damping coefficient of engine-mounting
c_{25} : Damping coefficient of frame-body
c_{eq} : Equivalent damping coefficient of stopper
d : Stopper clearance
$E[\ ]$: Expected value
F_d : Impact force on stopper
f_c : Corner frequency of shaping filter
k_1, k_4 : Stiffness of front and rear tires
k_2, k_5 : Stiffness of front and rear suspensions
k_3 : Stiffness of engine mounting
k_{eq} : Equivalent stiffness of stopper
L : Time delay between front and rear suspension
m_1, m_4 : Unsprung mass of front and rear suspension
m_2,m_5 : Sprung mass of front and rear suspension
m_3 : Engine-body mass
n : Index of deformation
$p(z_i)$: Probability density function of z_i
S : Road surface roughness
t : Time
V : Vehicle velocity
W_0 : One side power spectral density of white noise
$X_0(f)$: Power spectral density of road surface undulation
x_i : Displacement (i = 1, 2,....,5)
y : Relative displacement($y = x_3 - x_2$)
z_i : Random state variable (i = 1,2..12)
β : Stopper damping coefficient
κ : Stopper stiffness
σ_{Fd} : Standard deviation of F_d
σ_{xi}, σ_y : Standard deviation of x_i and y

3. Dynamic Model of Vehicle and Engine-mounting

3.1 Dynamic Model

The dynamic model of a vehicle and engine-mounting system with motion-limiting stops is shown in Fig.1. The engine-body m_3 is fixed on front sprung mass m_2 with stoppers having clearance d. The mass of engine body works as dynamic vibration absorber for a flexible frame-body structure(m_2, m_5, k_{25}, c_{25}). When the engine body vibrates under the action of impact force on motion-stoppers, the equations of motion are expressed as follows:

$$
\begin{aligned}
&m_1\ddot{x}_1 + c_2(\dot{x}_1 - \dot{x}_2) + k_1(x_1 - x_{01}) + k_2(x_1 - x_2) = 0 \\
&m_2\ddot{x}_2 + c_2(\dot{x}_2 - \dot{x}_1) - c_3\dot{y} + c_{25}(\dot{x}_2 - \dot{x}_5) + k_2(x_2 - x_1) - k_3 y + k_{25}(x_2 - x_5) = F_d \\
&m_2\ddot{y} + c_2(\dot{x}_1 - \dot{x}_2) + (1 + m_2/m_3)c_3\dot{y} + c_{25}(\dot{x}_5 - \dot{x}_2) + k_2(x_1 - x_2) \\
&\qquad + (1 + m_2/m_3)k_3 y + k_{25}(x_5 - x_2) = -(1 + m_2/m_3)F_d \\
&m_4\ddot{x}_4 + c_5(\dot{x}_4 - \dot{x}_5) + k_4(x_4 - x_{04}) + k_5(x_4 - x_5) = 0 \\
&m_5\ddot{x}_5 + c_5(\dot{x}_5 - \dot{x}_4) + c_{25}(\dot{x}_5 - \dot{x}_2) + k_5(x_5 - x_4) + k_{25}(x_5 - x_2) = 0
\end{aligned}
\tag{1}
$$

where F_d represents the transmitted impact force when either one of the stoppers receives a contact, and $y(= x_3 - x_2)$ is the relative displacement between the engine body m_3 and sprung mass m_2.

The road surface undulations x_{01} to the front tire and x_{04} to the rear can be obtained by

applying a shaping filter to Gaussian white noise, i.e.

$$\dot{x}_{01} + 2\pi f_c x_{01} = 2\pi f_c w(t), \qquad \dot{x}_{04} + 2\pi f_c x_{04} = 2\pi f_c u(t-L)w(t-L) \tag{2}$$

where $u(\ )$ denotes unit step function, f_c corner frequency of shaping filter, L time delay between front tire and rear tire, and $w(t)$ Gaussian white noise with its expected value zero. They are expressed as follows:

$$L = \frac{l_{wb}}{V} \tag{3}$$

$$E[w(t)] = 0, \quad E[w(t)w(\tau)] = W_0\delta(t-\tau) \tag{4}$$

where V represents vehicle velocity, l_{wb} wheel base and W_0 power spectral density, $\delta(\ )$ Dirac's delta function and $E[\ ]$ the expected value of [ ]'s.

3.2 Impact Model

In general, the impact force F_d takes the form of hysteresis loops as shown in Fig.2. This loop appears when the relative displacement $y(=x_3 - x_2)$ exceeds the clearance $\pm d$, i.e. $|y| > d$. The mathematical expression[3] of the impact force for motion stoppers can be given by:

$$F_d = \kappa(1+\beta\dot{y})(y-d)^n u(y-d) - \kappa(1-\beta\dot{y})(-y-d)^n u(-y-d) \tag{5}$$

where κ denotes stopper stiffness and $\kappa\beta(\pm y - d)^n$ damping factor to determine an energy loss on the contact surface during impact. The index n describes the deformation law during impact with its value from 1 to 1.5 to match the impact condition[3]. In this study, index n is assumed $n = 1$.

4. Theoretical Analysis

4.1 Equivalent Linear System

The impact force F_d is expressed as a nonlinear function of relative displacement y and velocity $\dot{y}$. We linearize the impact force , resulting in the equivalent linear damping force $c_{eq}\dot{y}$ and the equivalent linear restoring force $k_{eq}y$, i.e.

$$F_{deq} = c_{eq}\dot{y} + k_{eq}y \tag{6}$$

By introducing state variables $z_1 = x_1$, $z_2 = x_2$, $z_3 = y$, $z_4 = x_4$, $z_5 = x_5$, $z_6 = \dot{x}_1$, $z_7 = \dot{x}_2$, $z_8 = \dot{y}$, $z_9 = \dot{x}_4$, $z_{10} = \dot{x}_5$, $z_{11} = \dot{x}_{01}$ and $z_{12} = \dot{x}_{04}$, equation (1) and (2) can be expressed in the following expanded linear matrix form:

$$\dot{z}(t) = Az(t) + B_f w(t) + B_r u(t-L)w(t-L) \tag{7}$$

where $z(t) = [z_1, z_2, \ldots\ldots, z_{12}]^T$, A is the (12×12)'s expanded matrix, B_f and B_r the (12×1)'s column vector and $[\ ]^T$ denotes the transpose of [ ]'s.

4.2 Statistical Linearization of Impact Force

The values of c_{eq} and k_{eq} can statistically be determined by minimizing the mean-square error of difference between impact force F_d and its equivalent impact force F_{deq}. In the stationary stochastic process, c_{eq} and k_{eq} values are in general expressed as functions of responses[5], i.e.

$$c_{eq} = \frac{E[F_d z_8]}{E[z_8^2]}, \quad k_{eq} = \frac{E[F_d z_3]}{E[z_3^2]} \tag{8}$$

Assuming responses z_8 and z_3 as Gaussian probability distribution with its expected value zero, c_{eq} and k_{eq} values[4] can be obtained by integrating the terms $E[F_d z_8]$ and $E[F_d z_3]$ over the ranges $(-\infty \sim \infty)$ and $(-\infty \sim -d : d \sim \infty)$ as follows:

$$c_{eq} = 2\kappa\beta\left\{-\Phi\left(\frac{-d}{\sqrt{E[z_3^2]}}\right)d + \sqrt{\frac{E[z_3^2]}{2\pi}}\exp\left[\frac{-1}{2}\left(\frac{d}{\sqrt{E[z_3^2]}}\right)^2\right]\right\}, \qquad k_{eq} = 2\kappa\Phi\left(\frac{-d}{\sqrt{E[z_3^2]}}\right) \tag{9}$$

where $\Phi(\,)$ denotes commutative distribution function, i.e.

$$\Phi(U) = \frac{1}{\sqrt{2\pi}}\int_{-\infty}^{U}\exp\left(-\frac{\gamma^2}{2}\right)d\gamma \tag{10}$$

It can be seen from expression (9) that the equivalent damping coefficient and the stiffness are functions of the stopper clearance d and the response $E[z_3^2]$. In a special case of stopper clearance $d = 0$, c_{eq} and k_{eq} values are expressed in the reduced equations $c_{eq} = 2\kappa\beta\sqrt{E[z_3^2]/2\pi}$ and $k_{eq} = \kappa$. They approach zero as $d \to \infty$.

4.3 Moment Equation

The general solution of equation (7) is expressed as follows:

$$z(t) = \exp(At)z(0) + \int_0^t \exp[A(t-\tau)]B_f w(\tau)d\tau + \int_0^t \exp[A(t-\tau)]B_r u(\tau - L)w(\tau - L)d\tau \tag{11}$$

In the stationary process, the derivative of second-order moment $M(t)\left(= E[z(t)z^T(t)]\right)$ is zero, i.e.

$$\dot{M}(t) = E[\dot{z}(t)z^T(t)] + E[z(t)\dot{z}^T(t)] = 0 \tag{12}$$

In case of $t >> L$, Substituting equation (12) for equation (7), (11) and considering equation (4) derives the following moment equation.

$$AM + MA^T = -\left\{B_f B_f^T + B_r B_r^T + B_r B_f^T[\exp(AL)]^T + \exp(AL)B_f B_r^T\right\}W_0 \tag{13}$$

where A contains the equivalent damping coefficient c_{eq} and stiffness k_{eq} defined by equation (9). This gives a set of nonlinear equations for responses $E[z_i\ z_j]$ in terms of second-order moment . Each moment can be obtained by solving equation (13).

4.4 Impact Force

The statistics of impact force F_d for inputs with Gaussian probability distribution will now be obtained. Using the same approach as was used for the evaluation of c_{eq} and k_{eq}, the mean-square value $E[F_d{}^2]$ of impact force can be given by:

$$E\left[F_d^2\right] = 2\kappa^2\left(1+\beta^2 E\left[z_8^2\right]\right)\left\{\left(d^2 + E\left[z_3^2\right]\right)\Phi\left(\frac{-d}{\sqrt{E\left[z_3^2\right]}}\right) - \sqrt{\frac{E\left[z_3^2\right]}{2\pi}}\,d\exp\left[\frac{-1}{2}\left(\frac{-d}{\sqrt{E\left[z_3^2\right]}}\right)^2\right]\right\} \quad (14)$$

This response quantity can be calculated by substituting equation (14) for the values of $E[z_8{}^2]$ and $E[z_3{}^2]$ obtained from equation (13).

5. Analytical Results

Standard deviations $\sigma_{x2} = \sqrt{E\left[z_2^2\right]}$, $\sigma_y = \sqrt{E\left[y^2\right]}$, $\sigma_{Fd} = \sqrt{E\left[F_d^2\right]}$, and other responses can be expressed in terms of the system responses $E[z_i z_j]$ obtained from equation (13). Newton-Laphson is applied to solve this nonlinear equation.

To confirm the analytical results, the numerical simulation for the system equation (1) was conducted using Runge-Kutta-Gill. The white noise with Gaussian probability distribution is created with Box-Muller.

5.1 Numerical Model

To obtain the numerical data, the case of a 25 ton heavy-duty truck model with the following set of parameters will be considered as an example.

Heavy-duty-truck and stopper model

$m_1 = 600(kg)$, $k_1 = 3{,}430(kN/m)$, $m_2 = 4{,}450(kg)$, $k_2 = 667(kN/m)$

$c_2 = 4.96(kNs/m)$, $m_3 = 1{,}250(kg)$, $k_3 = 5{,}440(kN/m)$, $c_3 = 3.3(kNs/m)$

$k_{25} = 6{,}800(kN/m)$, $c_{25} = 0.618(kNs/m)$, $m_4 = 2{,}000(kg)$, $k_4 = 13{,}700(kNs/m)$

$m_5 = 16{,}700(kg)$, $k_5 = 5{,}880(kN/m)$, $c_5 = 19.8(kNs/m)$, $l_{wb} = 6(m)$

$\kappa = 100{,}000(kN/m)$, $\beta = 0.9(s/m)$, $d = 5,\ 10,\ 15\ (mm)$

Fig.3(a) shows frequency characteristics of the front sprung mass acceleration, when the front tire is exited with the sinusoidal wave of its amplitude $\pm 1(mm)$ for the dynamic model as shown in Fig.1. An experimental result is shown in Fig. 3(b), which obtained by exiting the vehicle using an elector-hydraulic shaker with the same condition as Fig.3(a). Sprung resonance appears around 2(Hz) followed by frame beaming resonance around 7 (Hz) and unsprung resonance around 13 (Hz). The two graphs are almost identical.

5.2 Random Responses

When a vehicle is traveling at velocity V, the power spectral density $X_0(f)$ of inputs x_{01} and x_{04} from the road surface undulation is generally expressed as follows[6]:

$$X_0(f) = (2\pi f)^{-2} SV \times 10^{-6} \ (m^2/H_z) \tag{15}$$

where S represents the intensities of the road surface roughness, i.e.

S = 2~8(m^3/c) : Very good, S = 8~32(m^3/c) : Good, S = 32~128(m^3/c) : Average
S = 128~512(m^3/c) : Poor, S = 512~2048(m^3/c) : Very poor

The desired input X_0 (f) can be obtained by applying a shaping filter defined as equation (2) to the white noise with its one side power spectral density $W_0 = X_0(f_c)$.

Fig.4 shows power spectral densities of the road surface undulation when the vehicle velocity is 50(Km / hr) and the corner frequency f_c = 0.1(Hz) which is set at small value compared with that of vehicle dynamics so that it won't affect responses. The solid thin line shows the power spectral density generated by applying the shaping filter to the white noise. The solid thick line represents the general expression (15). These densities are almost the same.

An example of the impact vibrations obtained by the digital simulation is depicted in Fig.5. Fig.5(a) shows the wave form of the relative displacement y and Fig.5(b) the impact force F_d.. It can be observed that the relative displacement is closely bound within the selected stopper clearance (=10 mm) and the impact force is created at the time of impact. The hysteresis loops of the displacement on Fig.5(a) and the force on Fig.5(b) are shown in Fig.5(c). It can be noted that the loops are kept within some boundary and show a stable energy dissipation by the impact motions.

Fig.6(a) shows the standard deviation σ_y of the relative displacement y as a function of the road surface roughness S using stopper clearance d as a parameter. The plain solid line represents the result obtained with the theoretical method and the solid line with circles the result by digital simulation. They are relatively in good agreement. It is noted that the motion limiting can be observed over $S \cong 20(m^3/c)$ ($\cong$ "Good") for the clearance d=5(mm), and $S \cong 200(m^3/c)$ ($\cong$ "Poor") for the clearance d=15(mm).

The standard deviation σ_{Fd} of the impact force is shown in Fig.6(b). It is noted that the impact force increases as the road surface roughness S rises. The theoretical result is in good agreement with that of simulation in higher road surface roughness. They do not very much coincide in smaller roughness. This is because of the infrequent impacts on stoppers in smaller road surface roughness. Small impact forces, however, are not important factor for the strength problem of the engine-mounting system. In case of "Very poor" (S=512~2,084(m^3/c)), very large impact forces are generated. The influence of the stopper clearance d is very little in this case. The two graphs provide useful data to estimate the strength problem of a engine-mounting system with motion-limiting stops in given road surface undulations. They indicate how much strength and stopper clearance need for the engine-mounting system.

As a typical example of other responses, the standard deviation σ_{z2} of the front sprung mass is shown in Fig.6(c). The theoretical result is in good agreement with that of digital simulation. It can be seen that the front sprung mass response is insensitive to stopper clearance.

Fig.7(a) and Fig.7(b) show how the equivalent stiffness k_{eq} and the equivalent damping coefficient c_{eq} vary depending on the road surface roughness. They increase as the road surface roughness rises. It can be observed that they consist of two different lines, infrequent impact and frequent impact, and become to $k_{eq} = \kappa$ and $c_{eq} = 2\kappa\beta\sqrt{E\left[z_3^2\right]/2\pi}$ as $S \to \infty$.

6. Conclusions

With this study, we proposed an approximate solution to the response of the engine-mounting system with motion-limiting stops for heavy-duty trucks when the stationary random inputs are applied to the vehicles. In order to calculate the response characteristics, we developed a mathematical model with the five degree-of-freedom system featuring nonlinearity in relative displacement and velocity between the engine body and the front sprung mass.

The moment equation for two random inputs with time delay has derived. The standard deviation of impact forces, relative displacements of front sprung and engine body masses have also been obtained theoretically and numerically. The results of digital simulation confirmed the theoretical results.

The impact force, the influence of the stopper clearance and other responses for given road surface roughness have been discussed in detail. This eventually led us to perform a successful estimation of the impact forces required when designing the engine-mounting system with motion-limiting stops for heavy-duty trucks.

References

(1)Inoh,T. and Aisaka,M., "Tuning techniques for Controlling Heavy-Duty Truck Shake-Vertical Tortional and Lateral", SAE. Paper No. 730650(1973)

(2)Araki.Y., et al., "Active Engine Mounting as Hybrid Dynamic Absorber for Truck-Shake", Proc. of 2nd Int. Conf. on Motion and Vibration Control(1994), 19

(3)Hunt,K.H., and Crossley,F.R.E., "Coefficient of Restitution Interpreted as Damping in Vibroimpact", Trans. ASME, J. App. Mech.42-2(1975),440

(4)Yokomichi,I, Aiska,M.,Araki,Y. and Inoh,T., "Stationary Random Oscillation of Engine-Mounting System with Motion-Limiting Stops", Trans. JSME(c), 63-608(1997),36

(5)Lin,Y.k., "Probability Theory of Structural Dynamics", MacGraw-Hill(1967)

(6)Yamakawa,S., "On Road Surface Undulation for Vehicle Tests", JSAE, 30-8, (1976), 656

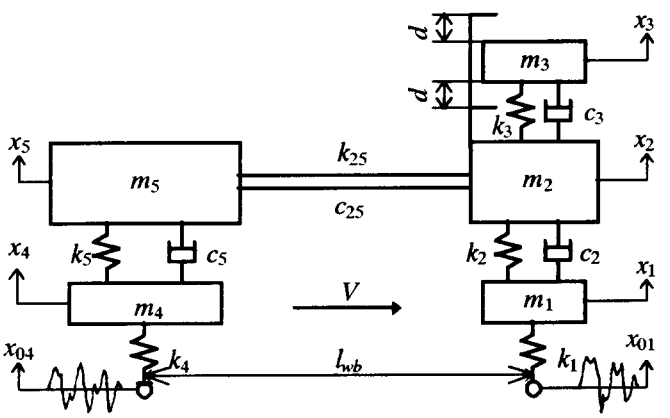

Fig.1 Dynamic model of vehicle with engine mounting with stopper.

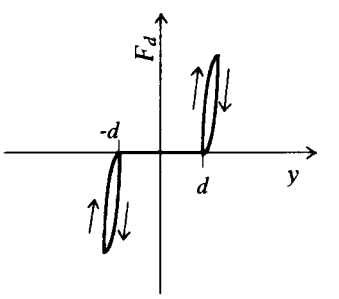

Fig.2 Force vs displacement characteristics of a typical impact.

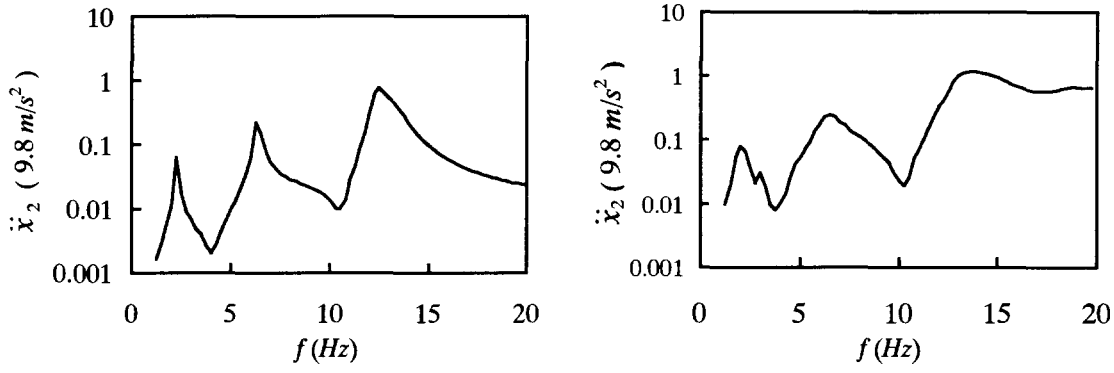

(a)Dynamic model. (b) Experiment.

Fig.3 Frequency characteristics of dynamic model and experiment when front tire excited.

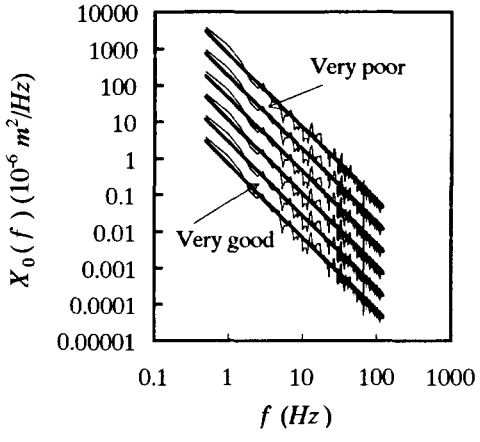

Fig.4 Power spectral density of road surface undulation.

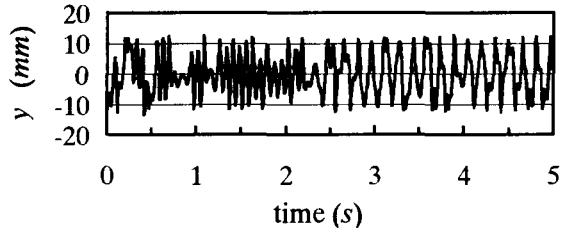

(a) Relative displacement y vs time.

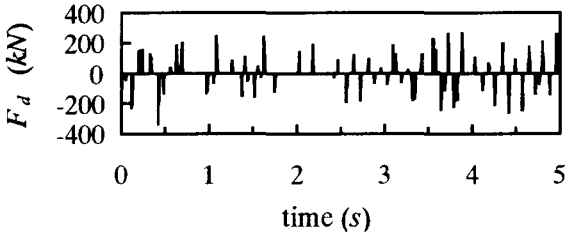

(b) Impact force F_d vs time.

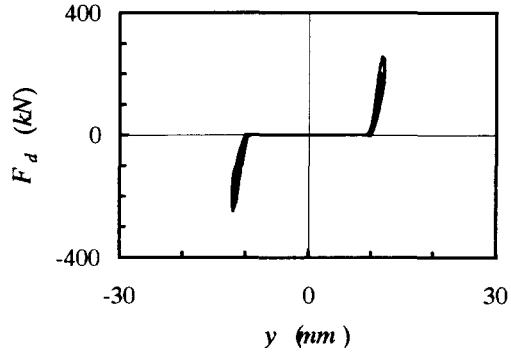

(c)Impact force F_d vs relative displacement.

Fig.5 Relative displacement and impact force in digital simulation (d=10 mm).

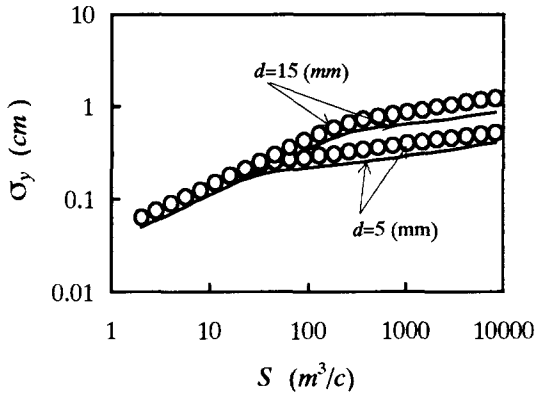

(a) Relative displacement of engine body.

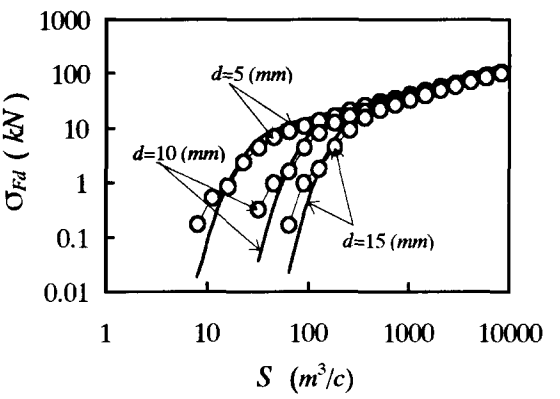

(b) Impact force.

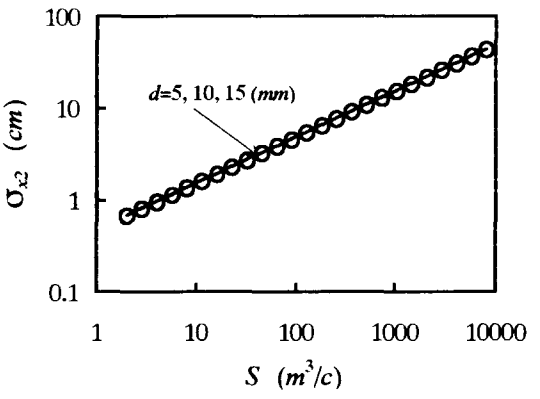

(c) Front sprung mass.

Fig.6 Standard deviation of response vs road surface roughness.

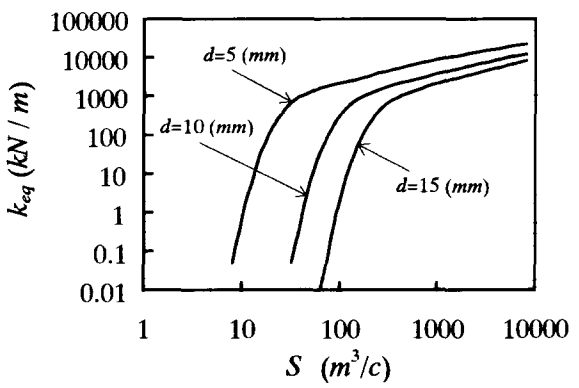

(a) Stiffness.

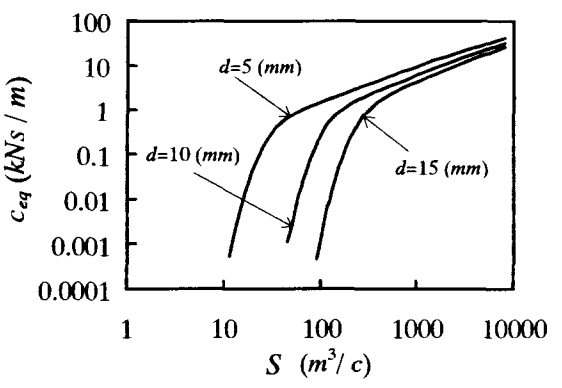

(b) Damping coefficient.

Fig.7 Equivalent linear stiffness and damping coefficient vs road surface roughness.